ELSEVIER

Polymer 41 (2000) 9191–9204

polymer

www.elsevier.nl/locate/polymer

Physical aging behavior of miscible blends containing atactic polystyrene and poly(2,6-dimethyl-1,4-phenylene oxide)

C.G. Robertson, G.L. Wilkes*

Chemical Engineering Department, Polymer Materials and Interfaces Laboratory, Virginia Polytechnic Institute and State University, Blacksburg, VA 24061, USA

Received 1 November 1999; received in revised form 28 February 2000; accepted 28 February 2000

Abstract

The influence of blend composition on physical aging behavior was assessed for miscible blends of atactic polystyrene (a-PS) and poly(2,6-dimethyl-1,4-phenylene oxide) (PPO). At aging temperatures of 15 and 30°C below the midpoint glass transition temperature (T_g), the a-PS/PPO blends exhibited volume relaxation rates that were retarded compared to additivity based upon the aging rates for pure a-PS and PPO. This negative deviation diminished with increased undercooling, and eventually the volume relaxation rates displayed a nearly linear trend with respect to composition at the greatest undercooling of 60°C that was employed. The compositional nature of unaged glassy density and secondary relaxation intensity, both influenced by the presence of specific attractive interactions in the blend system, were likely causes for the variation of volume relaxation rate with composition and undercooling. For aging at 30°C below T_g, the dependence of enthalpy relaxation rate on composition was similar to that observed for volume relaxation. Mechanical aging rates determined from time–aging time superposition of creep compliance data showed significantly less than additive behavior for the blends aged at $T_g - 30$°C, but unlike the volume relaxation results, this trend persisted at the 60°C undercooling.

Keywords: Miscible polymer blends; Physical aging; Volume

1. Introduction

The glassy state is inherently in nonequilibrium from a thermodynamic standpoint. During the cooling of a glass-forming liquid, the relative mobility of molecular segments becomes increasingly inhibited, in a manner which could be considered a molecular "log jam", and eventually a nonequilibrium glassy state is formed. The formation of the nonequilibrium glass occurs when the relaxation times become large relative to the time frame allowed for molecular rearrangements, a time frame dictated by the quench rate. Departure from equilibrium constitutes a driving force for relaxation in the glassy state and, consequently, decreases in the volume, enthalpy, and entropy occur due to localized molecular motion in the glassy state. The temporal changes in the thermodynamic variables of the glass are often termed structural relaxation and, considered together, result in a decrease in the free energy of the system. The changes that occur in the thermodynamic state, in turn, result in changes in numerous characteristics including mechanical, optical, and barrier properties. These property changes associated with the time-dependent nature of the glassy state have been described in great detail by several fine reviews [1–5]. The time-dependent nature of the thermodynamic variables in the glassy state (structural relaxation) as well as interrelated changes in bulk application properties are collectively referred to as physical aging. Because physical aging is a consequence of the non-equilibrium glassy state, it is thermoreversible unlike chemical or thermo-oxidative aging.

In principle, all materials can form an amorphous glassy phase if quenched rapidly enough from the liquid state to avoid complete crystallization. For polymer systems, achieving high crystal contents is not common, and many commercially important polymers are completely amorphous. Therefore, most polymeric materials that are used at temperatures below their glass transition temperature region possess significant glassy contents. In addition, relative to inorganic glasses, polymer glasses are often utilized at temperatures that are nearer to the glass transition temperature region where physical aging rates are significant. These factors combine to make physical aging of

* Corresponding author. Tel.: +1-540-231-5498; fax: +1-540-231-9511.

E-mail address: gwilkes@vt.edu (G.L. Wilkes).

0032-3861/00/$ - see front matter
PII: S0032-3861(00)00183-X

polymeric materials an important issue within the industrial community, and this research area has attracted much interest accordingly [5].

This research investigation is concerned with the nonequilibrium glassy behavior of miscible polymer blends. Because the nature of the glassy state formed from simple liquids is far from being completely defined, it may initially seem premature to probe the temporal nature of more complex multicomponent polymeric glasses. However, the research undertaken is timely for at least two reasons. From a practical standpoint, the use of polymer blends is becoming increasingly widespread for the purposes of developing economically viable materials with novel combinations of application properties. These properties of interest can undergo significant time-dependent changes (physical aging) below the glass transition due to the nonequilibrium nature of the glassy state. In addition, the introduction of complexities can provide a means of isolating the effects of certain molecular features on glassy state relaxations. For example, insight into the influence of intermolecular forces on the nonequilibrium behavior of the glassy state may be provided by the study of miscible polymer blend systems with specific interactions present between the blend components.

Physical aging of amorphous miscible polymer blends has been investigated to some extent [6–21], and an in-depth review of these investigations is provided elsewhere [22]. The majority of this past research was focused upon enthalpy relaxation/recovery measurements and none of the studies considered volume relaxation behavior. The goal of the present research study is to extensively investigate physical aging as a function of both blend composition and aging temperature for a widely studied, and commercially important, miscible blend system which is comprised of atactic polystyrene and poly(2,6-dimethyl-1,4-phenylene oxide). Both volume relaxation and enthalpy recovery measurements are included in this study in order to understand the time-dependent structural state for the blends and pure components. The degree to which the physical aging process induces changes in the small-strain mechanical creep response for the a-PS/PPO blend system is also an integral component of this investigation. Where possible, this study attempts to derive suitable interpretation of the aging results in terms of molecular-based concepts.

2. Experimental details

2.1. Blend preparation and characterization

Blends of atactic polystyrene (a-PS) and poly(2,6-dimethyl-1,4-phenylene oxide) (PPO) were prepared by mixing at 265°C for 15 min in a Brabender (Model 5501) melt mixer using a mixing speed of 70 rpm. A nitrogen purge was employed during the mixing process. Blends with compositions of 25, 50, 75, and 87.5 wt.% PPO were generated. The PPO material was obtained from Polysciences (Cat.# 08974) and has a weight-average molecular weight (M_W) of approximately 50,000 g/mol. The a-PS material employed in this study is produced by Dow Chemical (Dow 685D) and the number- and weight-average molecular weights for this polymer are 174,000 and 297,000 g/mol, respectively, as determined by gel permeation chromatography [23]. All polymer materials were dried under vacuum conditions at 70°C before blending. Films were compression molded from the neat materials and blends, and the resulting films had an approximate thickness of 0.2 mm. All materials were stored in a dessicator cabinet prior to testing. The inflection glass transition temperature (T_g) was investigated as a function of blend composition in a differential scanning calorimeter (Perkin Elmer DSC 7) for samples weighing 8–11 mg at a heating rate of 10°C/min following a quench from the equilibrium liquid state (T_g + 50°C) at 200°C/min (see *Enthalpy relaxation measurements* section for further DSC details). The breadth of the glass transition was also assessed for the blend system from the DSC scans. Density measurements were made at 23°C using a pycnometer manufactured by Micromeritics (Model AccuPyc 1330).

2.2. Enthalpy relaxation measurements

Prior to aging, samples weighing approximately 10 mg were loaded in aluminum pans and quenched into the glassy state at 200°C/min in the DSC after annealing at T_g + 50°C for 10 min. Samples were aged isothermally at T_g − 30°C (^ 0.5°C) in ovens under nitrogen purge for various amounts of time ranging from 1 to 300 h. Each sample was then scanned in the Perkin Elmer DSC 7 from T_g − 70°C to T_g + 50°C using a heating rate of 10°C/min (first heat). In order to provide an unaged reference with which to compare an aged DSC trace, each sample was then annealed in the DSC at T_g + 50°C for 10 min, quenched at 200°C/min, and scanned from T_g − 70°C to T_g + 50°C at 10°C/min (second heat). It was necessary to hold the DSC sample for 2 min at T_g − 70°C to allow control of the heat signal before initiation of the second heat. It is expected that this short amount of time, at this low temperature, has a negligible effect on the structural state of the sample. The extent of enthalpy recovery was determined from the first and second heating scans using two methods to be described later. A third heat was employed in some cases following annealing at T_g + 50°C for 10 min and quenching at 200°C/min. This third scan was performed in order to illustrate, by comparison with the second heat, the thermal stability of the material under the conditions employed during DSC testing. All DSC testing utilized a nitrogen purge. An instrument baseline was generated every 2 h of testing at a heating rate of 10°C/min using empty pans with lids in the reference and sample cells. The ice content in the ice/water bath was maintained at approximately 30–50% by volume during all testing. The DSC temperature was calibrated using the

melting points of indium and tin, and the heat flow was calibrated using the heat of fusion of indium.

2.3. Volume relaxation measurements

Isothermal volume relaxation was monitored for the a-PS/PPO blend system using a precision mercury dilatometry apparatus described in detail elsewhere [23]. Samples used were compression molded bar samples with weights in the range of 4–5 g (approximate dimensions: $1 \times 1 \times 4$ cm^3). After a sample was encased in the glass bulb of a capillary dilatometer, the dilatometer was placed under vacuum and was subsequently filled with mercury. A vacuum was placed on the filled dilatometer for approximately two days to remove any entrapped air bubbles, and the dilatometer was allowed to equilibrate at atmospheric pressure for one day following this de-gassing procedure. Just prior to volume relaxation measurements, the materials were annealed in the dilatometers for 10 min at $T_g + 50$°C using an oil bath and then quenched using an ice bath. The sample in the dilatometer was then isothermally annealed at the desired aging temperature in a Haake model N4-B oil bath with temperature control fluctuations less than 0.01°C. The height change of the mercury in the capillary was assessed as a function of aging time using a calibrated linear voltage differential transducer and converted to volume change based on the cross-sectional area of the capillary. The order of the undercoolings (relative to T_g) which were used for each blend sample was: 30, 60, 30, 15, 30, 45°C. After volume relaxation measurements were complete at one undercooling, the material was annealed 50°C above T_g and requenched into the glassy state where densification was followed at the next undercooling. The three experiments performed at $T_g - 30$°C allowed a measure of error to be obtained for the volume relaxation rate data.

The thermodynamic state of the quenched dilatometer samples was essentially identical to that of the quenched DSC samples used to assess enthalpy relaxation as was verified in the following manner. Films of a-PS were alternately stacked with Teflon® films to form a composite bundle with the approximate dimensions of a typical dilatometer sample, and this film bundle was encapsulated in a dilatometer bulb with mercury and de-gassed in the typical manner. The encased material was then annealed in the bulb at $T_g + 50$°C for 10 min and quenched to room temperature by immersion of the dilatometer bulb in an ice bath. Following this quench, the a-PS films were extracted from the bulb and then the outer and center layers were used to generate ~10 mg DSC samples. These samples were subsequently scanned in the DSC from $T_g - 70$°C to $T_g + 50$°C at 10°C/min, annealed at $T_g + 50$°C for 10 min, quenched at 200°C/min, and scanned a second time from $T_g - 70$°C to $T_g + 50$°C at 10°C/min. Fictive temperature (T_f) calculations were performed on both heating scans for the two film samples using the Perkin Elmer analysis software provided with the instrument. The first heats of the outer and center film samples provided T_f values of 103.5 and 103.0°C, respectively. The second heats for both samples yielded essentially equivalent fictive temperatures of 103.4°C, a value also obtained for a-PS samples which were freshly quenched (DSC quench at 200°C/min) and which were not previously subjected to enclosure in the dilatometer bulb. The issue is not whether the center of the dilatometry sample lags behind the surface of the sample during the quench into the glassy state because this is necessarily the case based upon heat transfer limitations. Of importance is the effective rate of cooling experienced by the sample during glass formation, and based upon the above study it is clear that the outside and center of the dilatometry sample experienced very similar rates of cooling. The center portion may have experienced a slightly lower cooling rate as evidenced by its lower T_f value compared to that for the center region, but this cooling rate discrepancy is certainly not very different on a logarithmic scale. The structural state generated upon glass formation depends on the logarithm of the cooling rate, and typical apparent activation energies lead to increases of 2–7°C in T_f with a ten-fold increase in cooling rate. Because the initial fictive temperatures generated by the DSC and dilatometry quenching conditions were comparable, the initial structural states of the samples were deemed essentially equivalent for the volume and enthalpy relaxation experiments.

2.4. Creep compliance testing

The influence of physical aging on tensile creep compliance behavior was assessed during isothermal aging. The testing was performed on initially unaged film samples which were freshly quenched after free-annealing at $T_g + 50$°C for 10 min. The small-strain creep response was probed after aging times of 1.5, 3, 6, 12, and 24 h using the procedure established by Struik [1]. A Seiko thermal mechanical analyzer (model TMA 100) was used to test the samples possessing the following approximate dimensions: 30 mm long, 0.2 mm thick, and 3 mm wide. The step stress applied to the samples during the creep measurements was kept small in order to insure that the total strain was kept well below 0.3% (the majority of total strain values were less than 0.15%). This enables a sample to be intermittently tested for its mechanical response during isothermal physical aging without the testing procedure significantly affecting the state of the sample after the stress is removed and the sample is allowed to recover. The total time during which the stress is applied is one-tenth of the total cumulative aging time, such that any aging which occurs during the creep test can be neglected.

2.5. Dynamic mechanical testing

Dynamic mechanical measurements (tensile) were made with a Seiko DMS 210 using samples (0.2 mm thick, 20 mm

Table 1
Glass transition temperature results

PPO content (wt.%)	DSC: 10°C/min heating scan following 200°C/min quench into glassy state				DMA: 1 Hz, 2°C/min heating	
	T_g (°C)	$T_{g,onset}$ (°C)	$T_{g,end}$ (°C)	$T_{g,start}$ (°C)	tan δ peak temp. (°C)	tan δ peak onset (°C)
0	103	100	106	92	121	103
25	127	122	132	115	146	127
50	149	142	155	134	169	147
75	170	164	177	154	195	172
87.5	195	189	200	179	217	195
100	215	211	218	201	229	212

long, 5 mm wide) which were freshly quenched after free-annealing at $T_g + 50$°C for 10 min. The testing procedure involved a heating rate of 2°C/min, a nitrogen purge, and a frequency of 1 Hz. The dynamic mechanical spectra were determined for the blends and pure polymers from −140°C to above the α-relaxation temperature region.

3. Results and discussion

Changes in the thermodynamic state of a glassy material during the physical aging process can be followed by directly monitoring volume changes using dilatometry or by inferring enthalpy changes by means of differential scanning calorimetry. Both of these approaches were employed in this investigation of the a-PS/PPO miscible blend system,

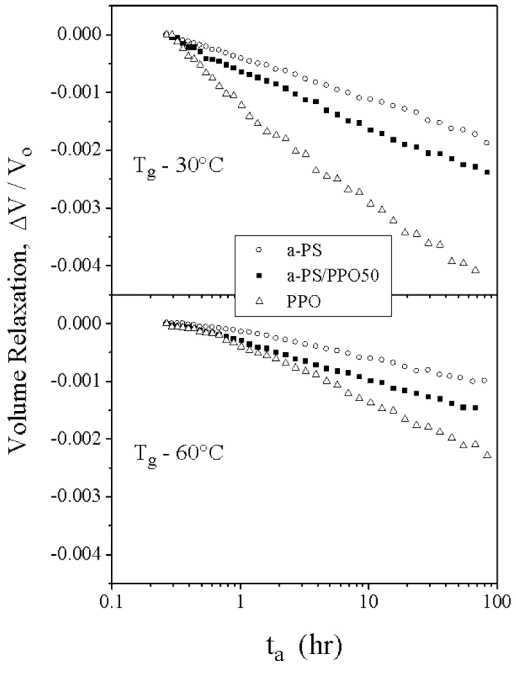

Fig. 1. Representative volume relaxation data at undercoolings of 30 and 60°C. An aging time of 0.25 h was used as the reference for determining volume differences (ΔV values). The negative slope of each data set represents the volume relaxation rate, b_V, and data points between 0.6 and 80 h were used in the rate determination.

and the results will be detailed and discussed. Compositional dependence of both dynamic mechanical response and glassy state packing will also be considered because these elements will provide some insight into the observed structural relaxation rate trends. Finally, the discussion will consider the mechanical response changes during physical aging as determined by creep compliance testing.

When considering the time-dependent glassy properties of miscible polymer blends and comparing them to the responses yielded by the pure constituents, the compositional dependence of T_g is an extremely pertinent issue. A valid comparison of physical aging rates for different glassy materials aged at a fixed temperature is not afforded when the glass transition temperatures are widely different. Atactic polystyrene and poly(2,6-dimethyl-1,4-phenylene oxide) have glass transition temperatures that are different by greater than 100°C, and, for the purpose of this study, aging rate comparisons are made at a fixed undercooling relative to the glass transition temperature which varies with blend composition. Glass transition results for the a-PS/PPO blends and the pure components are given in Table 1, and aging temperatures were selected relative to the inflection (midpoint) glass transition temperatures measured by DSC. The DSC glass transition data were obtained using a heating rate of 10°C/min immediately following a quench into the glassy state at 200°C, and, hence, these results reflect the responses for freshly quenched samples. Another important aspect to consider is the breadth of the glass transition for the blends, and this issue will be dealt with shortly.

3.1. Volume relaxation

The time-dependent nature of the thermodynamic state for a glassy material can be assessed by determining volume changes via dilatometry [24,25], and the densification of the blends and neat polymers was thus measured. Relaxation of volume in the glassy state is often found to display a linear dependence on log(time), a consequence of the nonlinear (self-limiting) nature of the structural relaxation process. With the exception of very short times and when the volume closely approaches the equilibrium volume (V_∞) at long times, isothermal volume relaxation at constant pressure can be described by the following expression, where b_V is

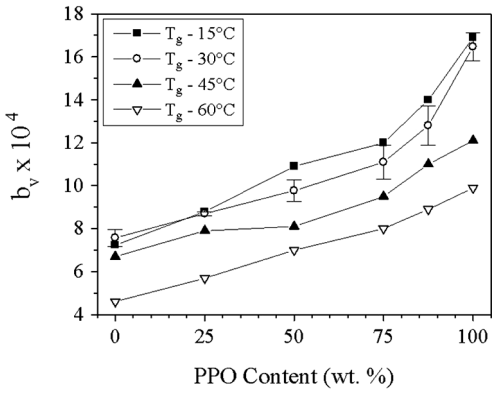

Fig. 2. Volume relaxation rate as a function of composition for the indicated undercoolings.

the volume relaxation rate [1,24]:

$$b_V = -\frac{1}{V}\frac{dV}{d\log t_a} \quad (1)$$

This approach is valid for isothermal volume relaxation following a fast quench or down-jump into the glassy state from the equilibrium liquid state, and this was essentially the experimental procedure employed for this study.

Isothermal volume relaxation was performed at temperatures equal to 15, 30, 45, and 60°C below T_g for each blend composition. Physical aging studies are often limited to temperatures less than 15°C below T_g because relevant time scales are experimentally amenable to characterizing relaxation all the way to equilibrium. However, glassy polymers are not typically used as rigid structural materials at temperatures so near to the glass-rubber softening temperature region. This research study undertook a practical approach and employed more realistic undercoolings. Representative volume-relaxation results are indicated in Fig. 1 for a-PS, PPO, and the 50/50 blend. Volume relaxation rates determined from the dilatometry data are provided for all of the compositions and undercoolings in Fig. 2. Inspection of the b_V data reveals interesting trends. The blend aging rates at $T_g - 15$°C and $T_g - 30$°C are clearly less than additive based upon the rates for pure a-PS and PPO. This negative deviation appears to diminish and eventually disappear upon aging at temperatures deeper in the glassy state. It does appear that a small degree of negative deviation is evident in the b_V versus composition data for the largest undercooling of 60°C but the trend is not statistically different than a linear relationship if the typical experimental error is taken into account. Forthcoming discussion will attempt to provide explanation for these features observed from the volume relaxation data.

An investigation of structural relaxation behavior of miscible a-PS/PPO blends was also undertaken by Oudhuis and ten Brinke [16], and these researchers assigned responsibility for the observed aging results to the heightened glass transition breadth for the blends. Their study followed isothermal annealing at a temperature 15°C below the onset-glass transition temperature, (as opposed to the midpoint-glass transition temperature used for reference purposes by the present authors). The authors qualitatively noted that the enthalpy relaxation was significantly slower for the blends relative to the pure components. The slower aging rates for the blends were attributed to concentration fluctuations in the blends, which caused broader glass transitions in comparison to the pure components. According to the authors, the significance of this glass transition breadth-difference between the blends and the pure polymers was that the blends, compared to pure a-PS and PPO, possessed regions that were further from the aging

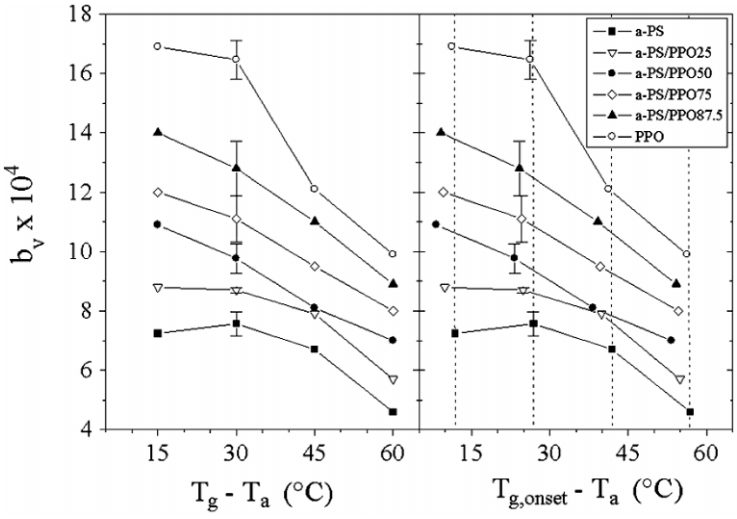

Fig. 3. Volume relaxation rates replotted as a function of undercooling. Both the midpoint and onset DSC glass transition temperatures are employed as references.

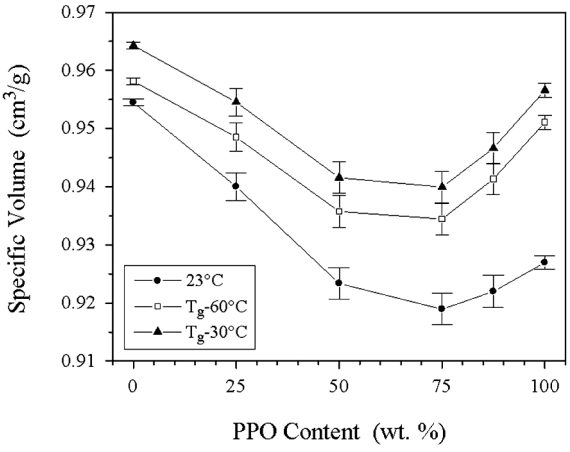

Fig. 4. Dependence of specific volume on blend composition for freshly quenched glassy samples.

temperature. It was reasoned that these less-mobile regions possessed longer relaxation times thus resulting in decreased overall structural relaxation rates for the blends compared to the pure homopolymers.

It now remains to test whether the retarded volume relaxation rates observed here for the blends at undercoolings of 15 and 30°C can be rationalized based upon the glass transition-breadth issue. Table 1 provides the experimental glass transition results for the a-PS/PPO blend system. Values of the onset ($T_{g,onset}$) and the end ($T_{g,end}$) temperatures of the DSC glass transition were determined via the standard technique which is employed by the instrument software. In addition, the start of the glass transition ($T_{g,start}$) was determined for each material, and this temperature represents the point where the first significant deviation from the glassy heat response occurs during heating. Because the $T_{g,start}$ values were of nearly equivalent distances below the respective $T_{g,onset}$ values for the blends and neat polymers, no advantage is given by using $T_{g,start}$ versus $T_{g,onset}$ for comparative scaling arguments. In order to determine the importance of the glass transition breadth, the volume relaxation rate data was scaled with respect to $T_{g,onset}$ as well as T_g. The contrasting b_V results are illustrated in Fig. 3. Applying interpolation/extrapolation to the data scaled relative to $T_{g,onset}$ (along the dotted lines), in order to obtain constant undercooling data, results in essentially the same trends exhibited in Fig. 2. Therefore, the presence of concentration fluctuations and their influence on glass transition breadth cannot be held responsible to any significant extent for the observed trends in volume relaxation rate.

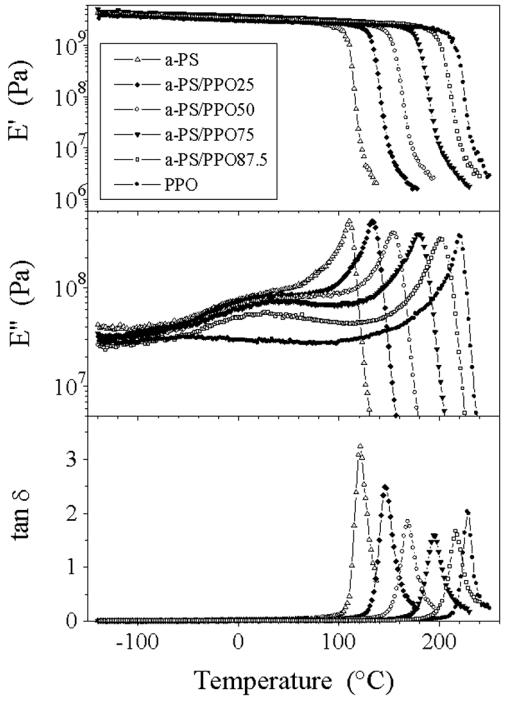

Fig. 5. Dynamic mechanical response for freshly quenched samples using a heating rate of 2°C/min and a frequency of 1 Hz.

An understanding of the negative deviation noted in the volume relaxation rate versus composition data can be gained by considering the glassy packing features of the blend system. The volumes of freshly quenched samples were measured using pycnometry at room temperature, and thermal expansion coefficients [26] were subsequently used to determine the state of packing as a function of composition at the undercoolings of 30°C and 60°C. The resulting specific volume results are plotted in Fig. 4, and it is apparent that the blends are much more densely packed in the glassy state compared to expectations based upon the densities of the pure components. This is, in fact, a well-established feature of this blend system [27,28]. This enhanced packing for the blends is a result of the interactions present between a-PS and PPO which modify the glass formation process during cooling. The nature of segmental cooperativity for the a-PS/PPO blends and its influence on glass transition kinetics is described in another publication [26]. Based upon the specific volume data, it is not surprising that the blends age slower than additive expectations at $T_g - 15$°C and $T_g - 30$°C. Prior to aging, the blends have less free volume than the neat polymers and intrinsically have lower mobility than additive behavior would suggest. This causes the initial volume decay for the blends upon annealing to be retarded relative to additivity, and this decay in turn causes the relaxation times to sharply increase further because the glassy structures are already quite highly packed for the blends. This suggests how the heightened state of packing for the a-PS/PPO blends can influence the self-limiting structural relaxation process. These arguments can explain the negative deviation observed in the b_V versus composition data for undercoolings of 15 and 30°C but cannot account for the change in the b_V trend which occurred upon aging at undercoolings which were deeper within the glassy state.

Inspection of dynamic mechanical responses for the blends and pure species can help illuminate the reason for the stark difference between the volume relaxation results at

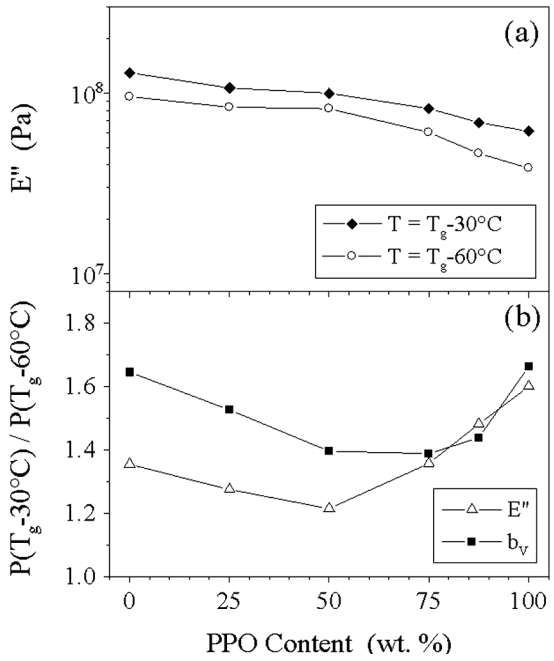

Fig. 6. Loss modulus at the indicated temperatures (a); and a comparison of property (P) ratios for loss modulus and volume relaxation rate. See text for additional details.

$T_g - 60$°C and those at $T_g - 30$°C. The dynamic mechanical spectra are given in Fig. 5 for all of the blend compositions investigated. Preliminary research indicated that the dynamic mechanical response of PPO is sensitive to moisture [22,29], and particular care was taken, therefore, to insure that all samples were thoroughly dry prior to testing. The compositional dependence of the glass transition temperature, and breadth thereof, can be observed from the spectra, and relevant parameters are listed in Table 1. The onset of the tan δ peak was arbitrarily defined for comparative purposes as the temperature at which the tan δ reached a value of 0.15 during heating. From the loss modulus data, a broad secondary relaxation is noted for pure PPO in the vicinity of −80°C (γ-relaxation) and atactic polystyrene displays a relaxation (β-relaxation) with a relatively low intensity at approximately 20°C. The locations of these sub-T_g relaxations are comparable to the findings of published studies [30–36]. Some reseachers [33,34] have additionally noted a weak β-relaxation for PPO between the α and γ processes. Similar to the results of this current study, Karasz and coworkers [35] did not observe the β-relaxation for PPO.

A comparison of the secondary relaxation responses evident for the blends with the sub-T_g behavior exhibited by pure a-PS and PPO is possible from the DMA data. Although the α-relaxation (glass-rubber softening transition) temperature region varies systematically with composition as expected, unusual behavior is present in this blend system with regard to secondary relaxations. It is apparent that the blends possess relaxation peaks in essentially the same temperature window where the secondary relaxation process occurs for a-PS, and, interestingly, this relaxation does not diminish with increasing PPO content to the extent that would be expected if only motion of a-PS is held responsible for the relaxation. An excellent dielectric study has been carried out on two a-PS/PPO blends containing 10 and 30 wt.% PPO by Monnerie and coworkers [9], and the intensity of the peak in the location of the β-relaxation for a-PS was found to increase with PPO content. PPO is substantially more dielectrically active than a-PS due to its greater polarity, and, hence, this dielectric analysis resulted in the important conclusion that PPO motion must accompany the movement of a-PS. Indeed, this cooperative behavior is most certainly responsible for the secondary relaxation behavior observed here by dynamic mechanical analysis. Again, specific attractive interactions between the different molecular species are playing a key role. It should be noted, however, that while the interactions modify the apparent strength of the secondary relaxation, the temperature-frequency location of the relaxation is not substantially affected.

It now remains to connect the secondary relaxation features evident in the blends to their structural relaxation behavior. Struik originally noted that the temperature dependence of volume relaxation rates appeared to qualitatively mimic the shape of the dynamic mechanical tan(δ) response with temperature, including local increases in aging rates with respect to temperature in the vicinity of secondary relaxations [37]. Therefore, the difference in the dynamic mechanical loss intensity (constant frequency) observed for one glassy temperature compared to another may be a semi-quantitative predictor of the relative rates of structural relaxation for the two temperatures. A comparison of the role of blend content on the dynamic loss modulus for undercoolings of 30 and 60°C is not overly informative as can be seen in Fig. 6a. The ratio of the loss modulus values at $T_g - 30$°C and $T_g - 60$°C does, however, appear to be a useful quantity, because a remarkable similarity is observed between the compositional dependence of this parameter and that observed for the ratio of volume relaxation rates (Fig. 6b). As was indicated previously, the dependence of glassy packing on blend content does not change in going from $T_g - 30$°C to $T_g - 60$°C (Fig. 4). The reduced mobility associated with the enhanced packing for the blends compared to that of a-PS and PPO may be counteracted at temperatures deep within the glassy state ($T_g - 60$°C) by the extra localized mobility in the blends associated with the unusual cooperative secondary relaxation behavior in the blends. This can explain the change in the b_V versus PPO content trend which occurred with increased undercooling. To reiterate the essential aspects of the preceding discussion, this investigation has developed a rationale for the observed dependence of volume relaxation rate on both blend composition and aging temperature. This rationale was developed by contrasting both the state of packing acquired upon glass formation and the sub-T_g-dynamic

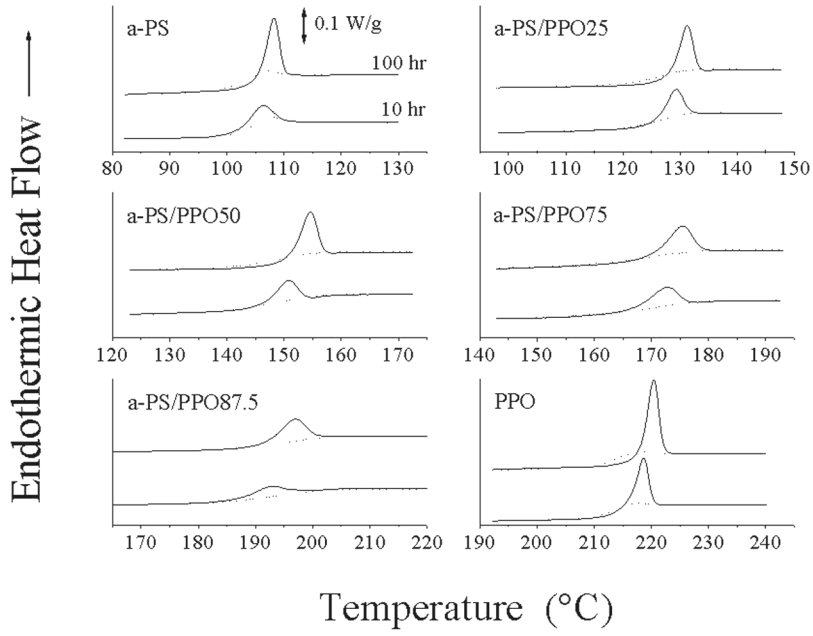

Fig. 7. Representative DSC enthalpy recovery traces during heating at 10°C/min following annealing at T_g − 30°C. The dotted lines represent the second heats after freshly quenching the samples into the glassy state at 200°C/min.

relaxation behavior of the blends with the respective characteristics of the pure species.

3.2. Enthalpy relaxation/recovery

Now that an adequate understanding of the volume relaxation data has been developed, it is useful to consider how the enthalpy relaxation process proceeds in comparison to the time-dependent behavior of volume for the blend system. Typical enthalpy recovery experiments were carried out following annealing for varied amounts of time at aging temperatures of T_g − 30°C and T_g − 60°C. Representative first and second DSC heating traces are indicated in Figs. 7 and 8 for the different blend compositions. Using the

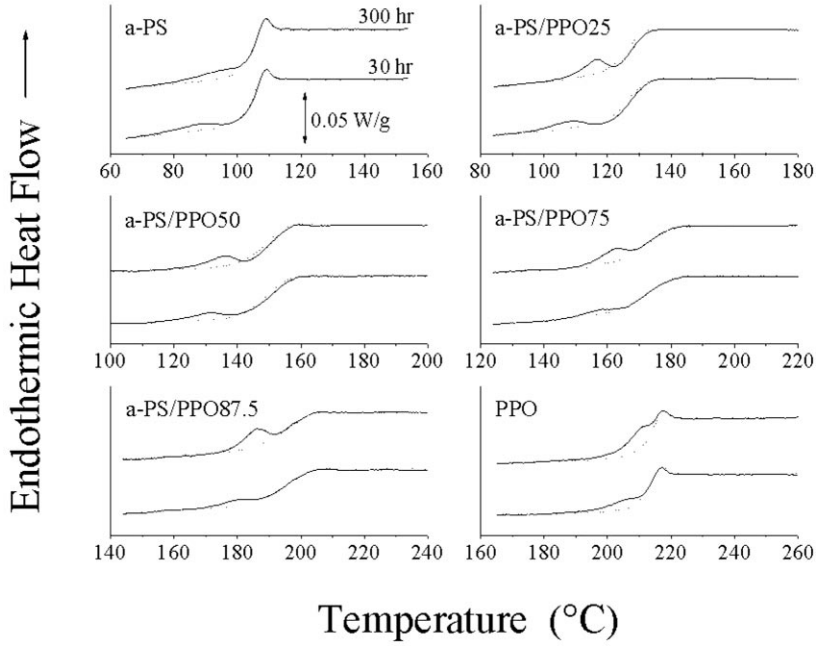

Fig. 8. Representative DSC enthalpy recovery traces during heating at 10°C/min following annealing at T_g − 60°C. The dotted lines represent the second heats after freshly quenching the samples into the glassy state at 200°C/min. Note that the scale is different than that used in Fig. 7.

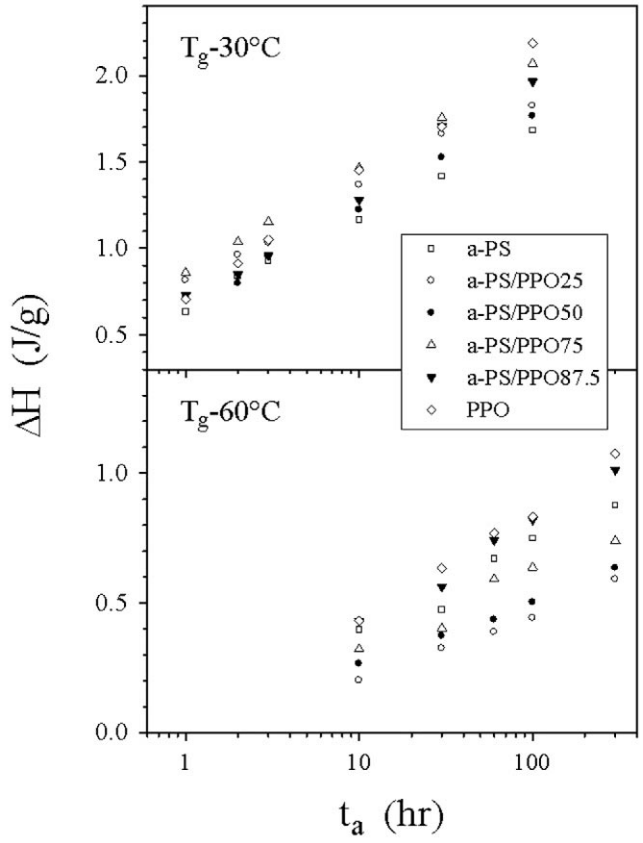

Fig. 9. Recovered enthalpy (ΔH) as a function of aging time for undercoolings of 30 and 60°C. Each data point represents the average ΔH from three DSC enthalpy recovery experiments.

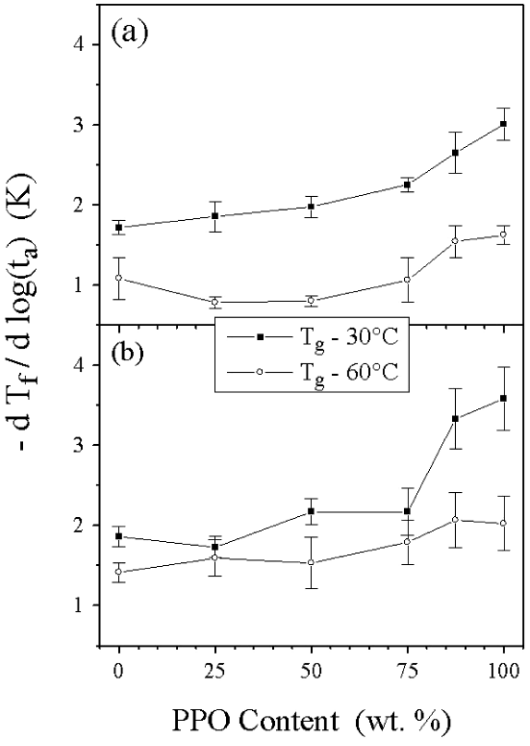

Fig. 10. Rate of change of enthalpic fictive temperature during aging. Rates were determined: (a) from the ΔH data; and (b) from the first heating scans using the software provided with the DSC instrument. See text for additional details.

standard subtraction procedure, values of the recovered enthalpy (ΔH) were determined, and it is assumed that these positive enthalpies represent the negative enthalpy changes which occurred during the aging interims. The enthalpy recovery results are given in Fig. 9.

As will become evident later, transforming the ΔH data into fictive temperature (T_f) results is informative. It is useful to have a parameter which quantifies the structural state of a glass, and a commonly utilized order parameter is the fictive temperature, T_f, introduced by Tool [38,39]. The fictive temperature is defined as the temperature at which the system would possess the equilibrium thermodynamic volume or enthalpy if instantaneously heated, a concept which is nicely illustrated in a review by Hutchinson [4]. During isothermal physical aging, the aging temperature (T_a) is constant but the structural, or fictive, temperature decreases toward T_a as structural relaxation progresses. The decrease in enthalpy during the annealing process can be simply related to the corresponding decrease in fictive temperature using the known difference between the liquid and glassy heat capacity for the material of interest. Assuming that the recovered enthalpy reflects the relaxed enthalpy, but with opposite sign, the following relaxation rate can be determined from the values of the slope ($d\Delta H/d\log(t_a)$) provided by the data in Fig. 9:

$$-\frac{dT_f}{d\log(t_a)} = \frac{1}{\Delta C_p}\frac{d\Delta H}{d\log(t_a)} \quad (2)$$

Consideration of the temperature dependence of ΔC_p is necessary in order to properly evaluate Eq. (2), and Table 2 provides the relevant data for the a-PS/PPO blend system. Using this approach, the relaxation rates were determined from the data given in Fig. 9 for aging temperatures of 30 and 60°C below T_g, and the results are provided in Fig. 10a. Discussion of this rate data will be undertaken shortly.

Another means of characterizing the enthalpy recovery response is by direct measurement of the fictive

Table 2
Observed differences between liquid and glassy heat capacities

PPO Content (wt. %)	$\Delta C_{p,g}$ (J/g K)	$\Delta C_p/\Delta C_{p,g}$ at $T_g - 30$°C	$\Delta C_p/\Delta C_{p,g}$ at $T_g - 60$°C
0	0.268	1.11	1.20
25	0.263	1.09	1.26
50	0.245	1.14	1.27
75	0.232	1.16	1.23
87.5	0.217	1.13	1.21
100	0.213	1.13	1.24

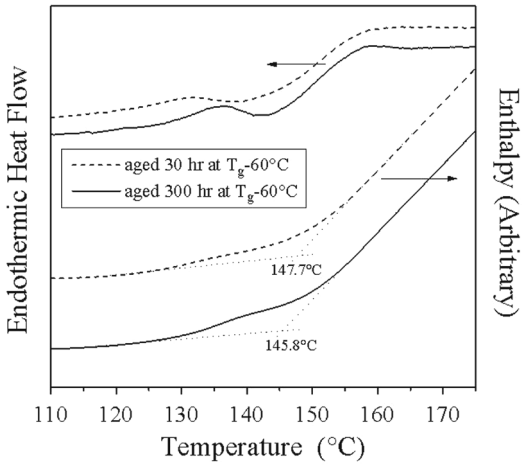

Fig. 11. Illustration of enthalpic fictive temperature assessment for a-PS/PPO50 blend aged at $T_g - 60°C$.

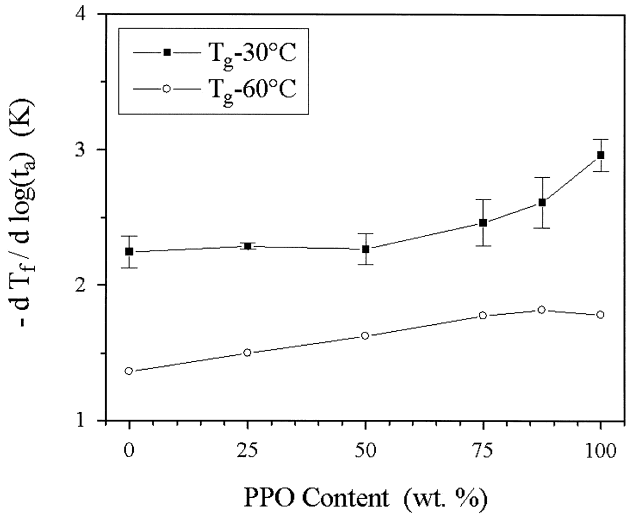

Fig. 12. Rate of change of volumetric fictive temperature during aging. See text for additional details.

temperatures from the enthalpy recovery DSC scans (first heats), using the DSC instrument analysis software. An example of the determination method employed by the software is illustrated in Fig. 11 for enthalpy recovery heating traces that were exhibited by the 50/50 blend. This technique enables relaxation rates ($-dT_f/d\log(t_a)$ values) to be determined, and these are given in Fig. 10b. Both analysis techniques provided similar trends in these rates with respect to blend composition at the aging temperature of $T_g - 30°C$, but notable differences are present at the undercooling of 60°C. At $T_g - 60°C$, the blends relax much slower than additive for the rates determined from the ΔH data while the direct determination of T_f values yielded essentially a linear trend with respect to composition. A possible source of this discrepancy becomes evident upon closer scrutiny of the enthalpy recovery DSC traces in Fig. 8. For the blends containing 25 and 50 wt.% PPO, the recovery curves undershoot the unaged reference scans (second heats) following the endothermic recovery bumps. Such undershoots were not apparent for samples which were annealed at $T_g - 60°C$ for short aging times, and the degree of undershoot appeared to become more pronounced with increased aging time. The cause for this very reproducible behavior is not known, but it leads to a reduction in the apparent recovered enthalpy, thus resulting in low recovery rates when the method employing the ΔH data is used. It is undeniable that caution must be exerted when interpreting recovery response and attempting to directly correlate it to the prior relaxation event. Following aging at $T_g - 60°C$, if the enthalpy recovery events for the a-PS/PPO25 and a-PS/PPO50 blends are atypically broad, particularly at the low temperature side of the pre-T_g endothermic peaks, these breadths may not be able to be discerned decently relative to the underlying glassy heat capacity responses. Some positive area may have been omitted, consequently, when integrating the curves generated by subtracting the reference scans from the recovery scans. Hence, the negative area associated with unusual undershoot behavior may not have been offset to the extent it should have been. The measurement of fictive temperatures may be a more appropriate methodology for materials, such as these blends, where the determination of ΔH appears to be problematic.

Determination of relaxation rates based upon changes in fictive temperature can also be assessed for volume. This can be accomplished by dividing the b_V values by the relevant jumps in thermal expansion coefficient at T_g, $\Delta\alpha$, values of which are given elsewhere [26]. Values of the volume relaxation rate ($-dT_f/d\log(t_a) = b_V/\Delta\alpha$) are plotted in Fig. 12 in order to compare with the rates determined for enthalpy. The rate trends are quite similar for volume and enthalpy at $T_g - 30°C$, irrespective of which technique was used to assess the enthalpy relaxation rate. For the undercooling of 60°C, the direct T_f calculation procedure appeared to provide enthalpy relaxation rates which exhibited a compositional dependence similar to that obtained for volume. A valid comparison of direct volume relaxation data with indirect enthalpy relaxation measurements can never be made without some question, particularly in this situation where very different trends result from the two distinct methods used to analyze the same enthalpy recovery data. However, based upon the above suggestion that the fictive temperature approach may be the best technique for indirectly assessing enthalpy relaxation, it appears as though volume and enthalpy display similar relaxation rates for the blend system at both undercoolings of 30 and 60°C.

3.3. Aging-induced changes in creep compliance behavior

In order to gain insight into the influence of the changing glassy structure on mechanical response for the a-PS/PPO blend system, small-strain creep compliance measurements were made as a function of aging time. Typical data are displayed in Fig. 13 for a-PS, PPO, and the 50/50 blend.

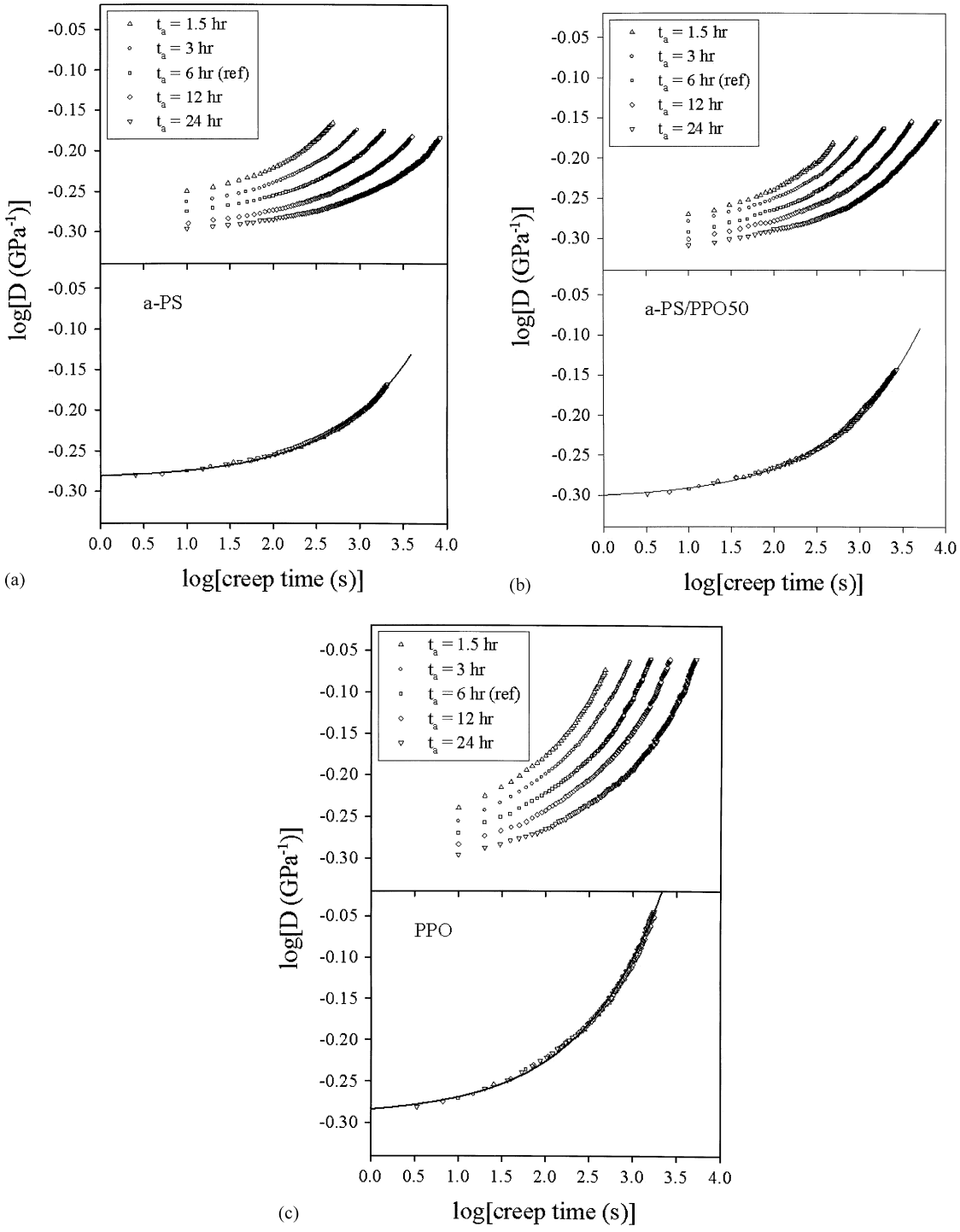

Fig. 13. Creep compliance responses for a-PS (a), a-PS/PPO50 (b), and PPO (c) aged at $T_g - 30°C$. Upper plots depict the data as a function of aging time, and the lower plots are the master curves generated at a reference aging time of 6 h as well as the stretched exponential fits to the master curve data. For clarity, only every fifth data point is included in the master curves.

Horizontal and vertical shifting were used in the typical manner to generate master curves, and time-aging time superposition appeared to be sufficiently valid for the blends and pure species. The degree of horizontal shifting can be used to determine a parameter, μ, which may be considered a mechanical aging rate, and this parameter is defined as [1]

$$\mu = \frac{\mathrm{d}\log(a_{t_a})}{\mathrm{d}\log(t_a)} \quad \text{where } a_{t_a} = \frac{\tau(t_a)}{\tau(t_{a,\mathrm{ref}})} \tag{3}$$

The compliance curve at an aging time of 6 h was

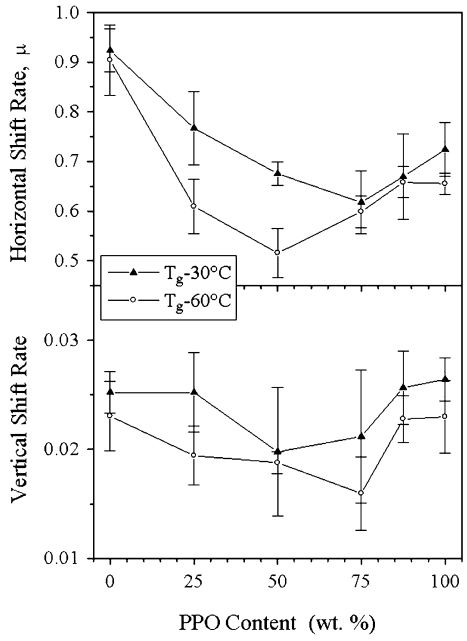

Fig. 14. Mechanical aging rates determined from horizontal and vertical shift factors used during formation of creep compliance master curves.

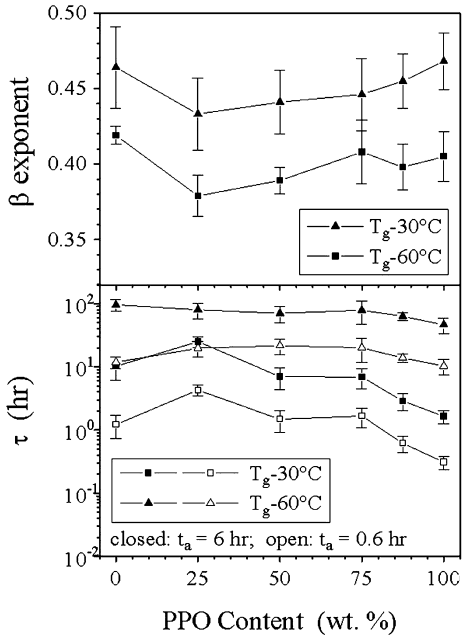

Fig. 15. Variation of the stretched exponential function parameters τ and β with composition for creep compliance response at $T_g - 30°C$ and $T_g - 60°C$.

selected as the reference, and the shift factor (a_{t_a}) was determined from the amount of shifting to the left on the log(time) axis which was required in order to superimpose a data set with the reference curve. The values of μ were subsequently determined, and these results along with the vertical shift rates are shown in Fig. 14. The dependence of μ on blend composition indicates that the blends age much slower than additive at both $T_g - 30°C$ and $T_g - 60°C$. It is difficult to state with extreme confidence that discernible trends are present in the vertical shift rate data because of the large error bars. It does appear as though the compositional trends for the vertical shift rates mimic, to a certain extent, the corresponding relationships observed between μ and PPO content.

Further analysis of the creep-compliance master curves can provide information concerning relaxation times and their breadth. The master curves were fit using the stretched exponential expression:

$$D(t) = D_0 \exp\left(\frac{t}{\tau}\right)^{\beta} \tag{4}$$

The τ parameter represents the most probable relaxation time for the reference aging time, and β provides a measure of the relaxation function breadth. Exponential relaxation is given by $\beta = 1$, and the relaxation function broadens as β decreases from this value towards zero. Because it is more useful to compare the relaxation times before any significant aging has occurred, the relaxation times determined from the fits were scaled back to an aging time of 0.6 h using the μ values. During ensuing discussion, the relaxation times at this short aging time of 0.6 h will be assumed to be representative of the initial creep compliance behavior prior to aging. The relaxation parameters are indicated in Fig. 15 as a function of aging time and undercooling. The relaxation time functions were broader for the blends in comparison to the pure polymers, and this is not surprising based upon the broader glass transition responses yielded by the blends. Also, the relaxation time function appears to broaden with increased undercooling for both the blends and neat homopolymers. This leads to the expectation that the relaxation time function also broadens with increased aging time for a given undercooling. Although time-aging time superposition may not be valid in the strictest sense because of this expectation, decent superposition of the data was apparent and the degree of shifting can still be informative. The role of composition on τ at $t_a = 0.6$ h indicates that the blends are inherently less mobile than additive for both undercoolings, and this is consistent with the negative deviation observed for the specific volume (unaged) versus composition data. The additional mobility which was manifested in the volume relaxation responses at $T_g - 60°C$ due to the cooperative secondary relaxations for the blends, as was previously hypothesized, apparently did not play a significant role in the unaged mechanical relaxation times for the blends compared to the influence of initial density features.

Although the dependence of the initial relaxation time on composition can be rationalized, the increases in the relaxation times during aging, which define the mechanical aging rates, show some unusual behavior. The negative deviation in μ with respect to composition at $T_g - 60°C$ is a peculiar result because the volume relaxation rates were essentially linear with PPO content at this undercooling. One of the

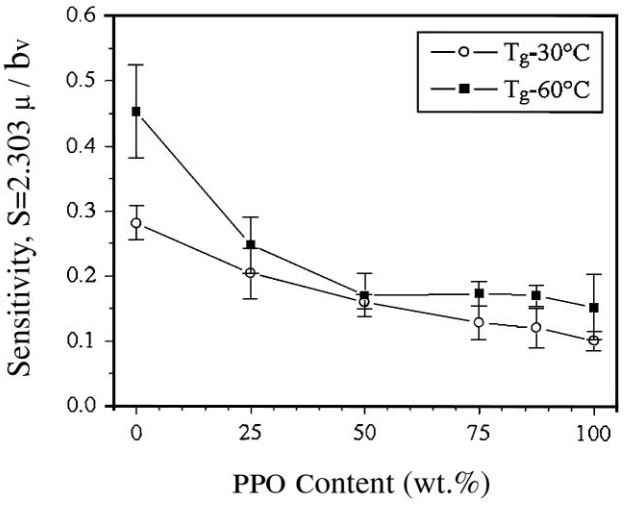

Fig. 16. Sensitivity of mechanical creep changes to structural volume changes for the blend system at undercoolings of 30 and 60°C.

characteristics which is often linked in a causal manner to mechanical mobility is free volume. A pertinent quantity is, therefore, the degree to which a reduction in volume affects the mechanical properties during aging. The sensitivity parameter, S, indicates the extent to which mechanical property changes are influenced by the changing structure [1]:

$$S = \frac{2.303\mu}{b_V} \tag{5}$$

Inspection of the variation of sensitivity with composition and undercooling in Fig. 16 reveals that the increase in sensitivity upon going from $T_g - 30°C$ to $T_g - 60°C$ is less than expected for the blends relative to the behavior of a-PS and PPO. As was stated earlier, no significant difference in the role of PPO content on the initial mechanical relaxation behavior was evident for an aging temperature of $T_g - 30°C$ compared to $T_g - 60°C$. The evaluation of the sensitivity parameter, however, revealed that the importance of aging-induced densification in dictating the degree to which the creep response shifts to longer times became noticeably diminished for the blends compared to additivity for aging performed deeper within the glassy state at $T_g - 60°C$.

4. Conclusions

The physical aging process was investigated as a function of blend composition and aging temperature for the a-PS/PPO blend system by employing volume relaxation, enthalpy relaxation/recovery, and creep compliance measurements. At aging temperatures of 15°C and 30°C below the midpoint glass transition temperature (T_g), the a-PS/PPO blends exhibited volume relaxation rates, which were retarded compared to additivity based upon the aging rates for pure a-PS and PPO. Broader glass transitions for the blends in comparison to a-PS and PPO were not responsible for this volume relaxation trend as was proven by rescaling the data with respect to the onset of the glass transition temperature. A heightened state of glassy packing for the blends was held responsible for the volume relaxation behavior at $T_g - 15°C$ and $T_g - 30°C$. The negative deviation in the volume relaxation data diminished with increased undercooling, and eventually the volume relaxation rates displayed a nearly linear trend with respect to composition at the greatest undercooling of 60°C which was employed. This change in trend is conjectured to be caused by a unique cooperative secondary relaxation process in the blends in the vicinity of the β-relaxation for a-PS which played more of an active role for aging performed deep in the glassy state. Enthalpy recovery experiments were performed following aging at undercoolings of 30 and 60°C, and two methods were used to analyze the data in order to infer the relaxation which occurred during the annealing process. Both techniques gave similar results for aging performed at $T_g - 30°C$, and the compositional dependence of enthalpy relaxation was similar to that observed for volume at this aging temperature. Due to unusual enthalpy recovery responses for the blends with 25 and 50 wt.% PPO following aging at $T_g - 60°C$, a discrepancy existed between the trends exhibited by the enthalpy relaxation data using the two methods. Therefore, a comparison of volume and enthalpy relaxation rates was inconclusive at the undercooling of 60°C. The variation of mechanical aging rate with composition exhibited a significant negative deviation from additivity, and this trend featuring substantially retarded aging rates was present at both undercoolings of 30 and 60°C which were investigated. The compositional dependence of glassy packing appeared to be the governing influence on the initial mechanical behavior prior to aging at both temperatures of $T_g - 30°C$ and $T_g - 60°C$. Strength for this argument was provided by the relaxation time parameters which were determined by fitting the creep compliance data. However, although the dependence of the initial mechanical response on the unaged state of packing for the blend system was similar for the undercooling of 30°C compared to 60°C, the sensitivity of mechanical property changes to the volume relaxation response was quite different for the blends at the two aging temperatures. The relaxation time distribution breadths inferred from the creep compliance master curves by stretched exponential fits applied to the data indicated that the blends possessed broader distributions than the pure components. This was consistent with glass transition breadths measured by both differential scanning calorimetry and dynamic mechanical analysis.

Acknowledgements

A research fellowship provided by Phillips Petroleum

Company and a summer fellowship supplied by Eastman Chemical Company are greatly appreciated.

References

[1] Struik LCE. Physical aging in amorphous polymers and other materials. New York: Elsevier, 1978.
[2] O'Reilly JM. CRC Critical Rev Solid State Mater Sci 1987;13:259.
[3] Tant MR, Wilkes GL. Polym Engng Sci 1981;21:874.
[4] Hutchinson JM. Prog Polym Sci 1995;20:703.
[5] McKenna GB. In: Booth C, Price C, editors. Polymer properties, Comprehensive polymer science, 2. Oxford: Pergamon, 1989. p. 311–62 chap. 10.
[6] Prest WM Jr, Luca DJ, Roberts FJ Jr. In: Thermal Analysis in Polymer Characterization Turi EA (Ed.), Heyden, PA, 1981. p. 24–42.
[7] Prest Jr WM, Roberts Jr FJ. In: Miller B, editor. Thermal analysis. Proceedings of the seventh international conference on thermal analysis, 2. New York: Wiley, 1982. p. 973–8.
[8] Cavaille JY, Etienne S, Perez J, Monnerie L, Johari GP. Polymer 1986;27:686.
[9] Pathmanathan K, Johari GP, Faivre JP, Monnerie J. Polym Sci, Part B: Polym Phys 1986;J24:1587.
[10] Bosma M, ten Brinke G, Ellis TE. Macromolecules 1988;21:1465.
[11] Cowie JMG, Ferguson R. Macromolecules 1989;22:2312.
[12] Mijovic J, Ho T, Kwei TK. Polym Engng Sci 1989;29:1604.
[13] Ho T, Mijovic J. Macromolecules 1990;23:1411.
[14] Elliot S. PhD dissertation, Heriot-Watt University, UK, 1990.
[15] Ho T, Mijovic J, Lee C. Polymer 1991;32:619.
[16] Oudhuis AACM, ten Brinke G. Macromolecules 1992;25:698.
[17] Pauly S, Kammer HW. Poly Net Blends 1994;4:93.
[18] Chang G-W, Jamieson AM, Yu Z, McGervey JD. J Appl Polym Sci 1997;63:483.
[19] Campbell JA, Goodwin AA, Mercer FW, Reddy V. High Perform Polym 1997;9:263.
[20] Cowie JMG, McEwen IJ, Matsuda S. J Chem Soc, Faraday Trans 1998;94:3481.
[21] Cowie JMG, Harris S, Gomez Ribelles JL, Meseguer JM, Romero F, Torregrosa C. Macromolecules 1999;32:4430.
[22] Robertson CG. PhD dissertation, Virginia Polytechnic Institute and State University, 1999.
[23] Shelby MD. PhD dissertation, Virginia Polytechnic Institute and State University, 1996.
[24] Greiner R, Schwarzl FR. Rheol Acta 1984;23(4):378.
[25] Marvin RS, McKinney JE. In: Mason WP, editor. Physical acoustics, II. New York: Academic Press, 1965.
[26] Robertson CG, Wilkes GL. Glass formation kinetics for miscible blends of polystyrene and poly(2,6-dimethyl-1,4-phenylene oxide), Journal of Polymer Science: Part B: Polymer Physics, submitted for publication.
[27] Hopfenberg HB, Stannett VT, Folk GM. Polym Engng Sci 1975;15:261.
[28] Kleiner LW, Karasz FE, MacKnight WJ. Polym Engng Sci 1979;19:519.
[29] Robertson CG, Wilkes GL. In: Tant MR, Hill AJ, editors. Structure and Properties of Glassy Polymers, Washington DC: ACS, 1998. p. 133.
[30] Chung CI, Saur JA. J Polym Sci, Part A-2 1971;9:1097.
[31] Illers KH, Jenckel E. J Polym Sci 1959;41:528.
[32] Yano O, Wada Y. J Polym Sci, Part A-2 1971;9:669.
[33] Yee AF. Polym Engng Sci 1977;17:213.
[34] De Petris S, Frosini V, Butta E, Baccaredda M. Makromol Chem 1967;109:54.
[35] Karasz FE, MacKnight WJ, Stoelting J. J Appl Phys 1970;41:4357.
[36] Ko J, Park Y, Choe S. J Polym Sci, Part B: Polym Phys 1998;36:1981.
[37] Struik LCE. Polymer 1987;28:1869.
[38] Tool AQ. J Am Ceram Soc 1946;29:240.
[39] Tool AQ. J Res Natl Bur Stand 1946;37:73.